CR-189329

CORRELATIVE ANALYSIS OF HARD AND SOFT X-RAY OBSERVATIONS OF SOLAR FLARES

A FINAL REPORT

NAS5-32064

Submitted to:

NASA/GSFC Greenbelt, MD 20771

Submitted by:

Dominic M. Zarro
Applied Research Corporation,
8201 Corporate Dr. Landover, MD 20785.

Date:

January 21, 1994

1. INTRODUCTION

This report discusses results of work performed under the Phase 2 Compton Gamma-Ray Observatory (CGRO) Guest Investigator Program. The goal of this work is to study different solar flare models by comparing their predictions with simultaneous high-spectral sensitivity hard and soft X-ray observations. We have used hard X-ray observations from the CGRO Burst and Transient Source Experiment (BATSE) and soft X-ray observations from the Bragg Crystal Spectrometer (BCS) on the Japanese Yohkoh spacecraft.

We have been analyzing solar flares that show evidence for strong stationary Ca XIX emission at the start of impulsive hard X-rays. An example is the M3.3 event that occurred at 0857 UT on 1992 September 6 in Active Region AR 7270. Figure 1b in the attached Appendix shows the evolution of hard X-rays (> 50 keV) for the event as detected in one of the sunward-facing Large Area Detectors (LAD) on BATSE. Significant HXR emission was first detected at 09:02 UT and reached a maximum at 09:03:31 UT. Figure 1a shows the BCS Ca XIX spectrum nearest the onset of hard X-rays at 09:01:57 UT. The Ca XIX profile was dominated by a strong component at the rest wavelength of the resonance line.

2. WORK PERFORMED

The observation of strong stationary soft X-ray emission before the peak of hard X-rays is a controversial result that cannot be readily explained by conventional flare models such as the thick-target electron-beam model. A model that can potentially explain the preflare heating necessary to produce significant Ca XIX emission and the electron acceleration required to produce nonthermal hard X-rays is the DC-electric field model (Holman 1985, Ap.J., 293, 584). In this model, oppositely-directed current filaments are aligned parallel to the direction of the coronal magnetic field. These currents heat the corona, while the DC-electric field associated with the currents produce high-energy electrons by runaway acceleration.

To test this model, we have performed the following analysis:

- scanned the Yohkoh and CGRO archives for strong solar flares for which there were joint BATSE and BCS observations of the preflare and impulsive phases;
- derived the hard X-ray emission above 50 keV for each flare from the LAD high-energy channels. To a first approximation, the hard X-ray emission is proportional to the rate of electron acceleration;
- fit single- and double-component power-law models to the LAD CONT and SD SHERB spectral data to look for evidence of spectral breaks. Spectral breaks are an indicator of electric-field acceleration processes. Evidence for a spectral break near 40 keV was found in the flare of 6 September 1992;

• computed temperature and density histories for each flare by fitting spectral models to the soft X-ray Ca XIX spectra. The temperature and density permit a derivation of the thermal heating rate Q_{obs} that sustains the soft X-ray emission;

• developed the following novel technique for combining the BATSE and BCS data in a test of the DC-electric field model. In the DC-electric field model, the ratio of the electron runaway rate $\dot{N}$ to the thermal heating rate Q is a function of temperature T, electron density n, and electric field strength E:

$$\dot{N}/Q = 2.5 \times 10^8 T_7^{-3/2} (E_D/E)^{19/8} \times \exp[(\mathrm{E_D}/2\mathrm{E})^{1/2} - (\mathrm{E_D}/4\mathrm{E})] \quad (1),$$

where $E_D \simeq 7 \times 10^{-6} n_9 T_7^{-1}$ is the Dreicer electric field, which is the electric field strength for which all thermal electrons undergo runaway accleration. The above ratio has the useful property that it is dependent only on T, n, and E. In particular, given observational measurements of T and n, this ratio provides a novel diagnostic of the unknown electric field strength.

To derive E, we relate the BATSE hard X-ray flux above 50 keV to $\dot{N}$ by a constant of proportionality α. We then perform a least-squares fit of the observed ratio of rates to the above theoretical ratio:

$$F_{HXR}/Q_{obs} \simeq \alpha \dot{N}/Q \quad (2).$$

This analysis has yielded the following results:

- the overall evolution of the BATSE hard X-ray and the BCS soft X-ray emissions can be explained by a current heating and electric field acceleration model;
- the initial increase in hard X-ray emission is consistent with a DC-electric field strength that increases from a preflare value of $E \lesssim 10^{-5}$ volts cm^{-1} to a peak value of $E \simeq 9 \times 10^{-5}$ volts cm^{-1}, which remains constant during the impulsive phase. Figure 1b (Appendix) compares the hard X-ray emission predicted by the above model with the BATSE observations. The evolution of the derived electric field is shown in figure 1c.
- the decrease in hard X-ray emission after flare maximum is consistent with an increase in coronal density. The increased density acts to quench the runaway process by enhancing collisional thermalization of the electrons.

4. SUMMARY

We have developed a promising new technique for jointly analyzing BATSE hard X-ray observations of solar flares with simultaneous soft X-ray observations. The technique is based upon a model in which electric currents and associated electric fields are responsible for the respective heating and particle acceleration that occur in solar flares. A useful by-product of this technique

is the strength and evolution of the coronal electric field. The latter permits one to derive important flare parameters such as the current density, the number of current filaments composing the loop, and ultimately the hard X-ray spectrum produced by the runaway electrons.

We are continuing to explore the technique by applying it to additional flares for which we have joint BATSE/Yohkoh observations. A central assumption of our analysis is the constant of proportionality α relating the hard X-ray flux above 50 keV and the rate of electron acceleration. For a thick-target model of hard X-ray production, it can be shown that α is in fact related to the spectral index and low-energy cutoff of precipitating electrons. The next step in our analysis is to place observational constraints on the latter parameters using the joint BATSE/Yohkoh data.

We have presented preliminary results of our work at the Yohkoh symposium: "A New Look at the Sun", that was held in Kofu, Japan in August 1993. The proceedings of this symposium are in the accompanying Appendix. We have also presented results at the Solar Physics Division meeting in Stanford, CA in July 1993, and the American Astronomical Society meeting in Washington, DC in January 1994. We are currently completing a paper for submission to the *Ap.J. (Letters)*.

STUDYING SOLAR FLARES WITH YOHKOH AND THE COMPTON GAMMA-RAY OBSERVATORY

Dominic ZARRO
Solar Data Analysis Center, Code 682, NASA/GSFC, Greenbelt, MD 20771
John MARISKA
Naval Research Laboratory, Code 7673, Washington, DC 20375
Brian DENNIS
Laboratory for Astronomy and Solar Physics, Code 682.2, NASA/GSFC, Greenbelt, MD 20771

Abstract

We apply a DC-electric field model to the analysis of soft and hard X-ray observations of a solar flare observed by *Yohkoh* and the *Compton Gamma-Ray Observatory* on 1992 September 6. The flare was observed in Ca XIX by the *Yohkoh* Bragg Crystal Spectrometer (BCS) and simultaneously in hard X-rays by the CGRO Burst and Transient Spectrometer Experiment (BATSE). A strong stationary component of Ca XIX emission was observed at the start of impulsive hard X-ray emission indicating an extended phase of heating prior to the production of energetic nonthermal electrons. We interpret the preflare Ca XIX emission as a signature of Joule heating by field-aligned currents. We relate the temporal variation of impulsive hard X-ray emission to the rate of runaway electron acceleration in the same DC-electric field.

1. Introduction

Electric currents and their associated electric fields provide a viable mechanism for heating and accelerating particles in solar flares (Holman 1985; Moghaddan-Taaheri and Goertz 1990; Benka and Holman 1992). In particular, quasi-static DC-electric fields parallel to the coronal magnetic field can accelerate thermal electrons until a steady-state current is established. Since the collisional drag on the electrons decreases with increasing velocity, a fraction of the current electrons above a critical velocity will undergo runaway acceleration to superthermal energies (Dreicer 1959; Spicer 1982). These runaway electrons can produce significant nonthermal hard X-ray (HXR) emission via thick-target interactions (Holman, Kundu, and Kane 1989). Electrons with velocities below the threshold for runaway acceleration continue to provide energy to the ambient plasma (via Joule heating) producing thermal soft X-ray

emission. Hence, an attractive feature of electric fields is their potential for simultaneously explaining thermal and nonthermal processes occurring in solar flares.

This paper explores the observational consequences of a DC-electric field model for the behavior of soft and hard X-ray emission in a solar flare. We report new results obtained by applying a DC-electric field model to simultaneous soft and hard X-ray observations of a flare obtained by instruments onboard the *Yohkoh* and *Compton Gamma-Ray Observatory (CGRO)* spacecraft.

2. Observations

A *GOES*-class M3.3 flare occurred at 0857 UT on 1992 September 6 in Active Region AR 7270 located at S11 W38. It was observed in the soft X-ray Ca XIX (3.17 Å) line by the Bragg Crystal Spectrometer (BCS) and simultaneously in hard X-rays by the *CGRO* Burst and Transient Source Experiment (BATSE). Figure 1a shows the BCS Ca XIX spectrum nearest the onset of hard X-rays at 09:01:57 UT. The Ca XIX profile was dominated by a strong component at the rest wavelength of the resonance line. This component was detected first at 08:58 UT and continued to increase in strength during the impulsive phase. Figure 1b shows the evolution of hard X-rays (> 50 keV) for the event as detected in one of the sunward-facing Large Area Detectors (LAD) on BATSE. Significant HXR emission was first detected at 09:02 UT, and increased to a maximum at 09:03:31 UT.

We derive the characteristic temperature T and emission measure EM ($= \int n^2 dV$) of the flare plasma from least-squares fitting of model spectra to the Ca XIX profiles. Figure 1b shows the fitted spectrum plotted over the observed preflare spectrum. The Ca XIX observations indicate a preflare temperature of 10×10^6 K increasing to a maximum of 20×10^6 K. The emission measure increased from a preflare value of 5×10^{47} cm^{-3} to a maximum of 4×10^{49} cm^{-3}. The Ca XIX profile also showed a blue-asymmetry during the rise phase of hard X-rays. We fit the blue-asymmetry by including a second blueshifted Ca XIX profile in the least-squares analysis. From the separation of the stationary and blueshifted components, we derive a line-of-sight upflow velocity of $\approx$ 260 km s^{-1} at the start time of hard X-rays. The upflow velocity was largest at the start of hard X-rays and decreased gradually during the flare. The soft X-ray blueshift and increase in emission measure suggest that the density in the loop increased as the result of chromospheric evaporation.

We use Be-filter images from the *Yohkoh* Soft X-ray Telescope (SXT) to infer the geometry of the flare region. The Be images indicate that the flare soft X-ray emission commenced in a single symmetric loop structure with a semi-circular half-length of $L \simeq 8 \times 10^8$ cm. As the flare progressed, the entire loop structure brightened simultaneously with the increase in Ca XIX emission. The soft X-ray emission was brightest at the apex before the start of impulsive hard X-rays. The emission was confined initially to $\approx$ 5 high resolution SXT pixels, corresponding to a cross-sectional area of $A \simeq 1.6 \times 10^{17}$ cm^2. We identify this area as the source of the preflare Ca XIX emission.

3. Analysis

In the DC-electric field model, the ratio of the electron runaway rate $\dot{N}$ (electrons s^{-1}) to the Joule heating rate Q (ergs s^{-1}) is given by (Holman, Kundu, and Kane 1989):

$$\dot{N}/Q = 2.5 \times 10^8 T_7^{-1} (E_D/E)^{19/8} \times exp[-2^{1/2}(E_D/E)^{1/2} - (1/4)(E_D/E)] \qquad (1)$$

In the above, E (volts cm^{-1}) is the electric field strength and $E_D \simeq 7 \times 10^{-8} n_9 T_7^{-1}$ is the Dreicer electric field. The numerical subscripts denote the order of each parameter (e.g., $T_7 = T/10^7$, etc). The above ratio has the useful property that it is dependent only on T, density

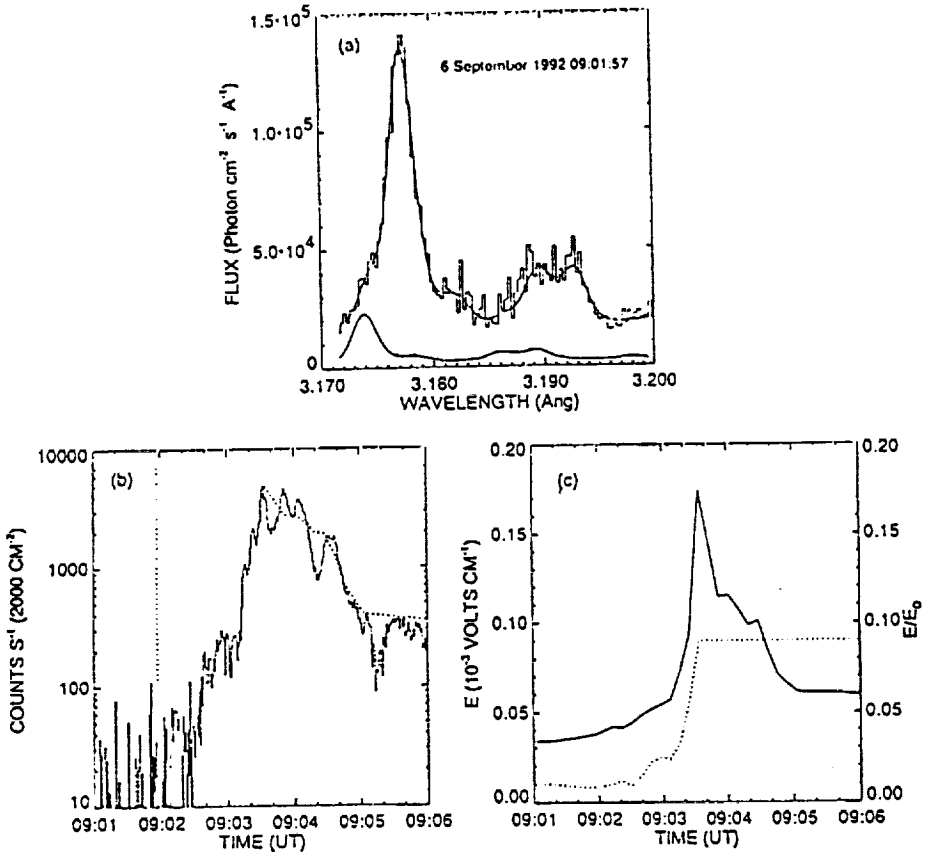

Fig. 1. Panel (a): preflare BCS Ca XIX spectrum (15 s accumulation time) showing fitted stationary and blueshifted components. Panel (b): comparison between background-subtracted BATSE HXR emission (1.024 s) above 50 keV (histogram) with the prediction made by the DC-electric field model (dotted line). Vertical dotted line marks time of preflare Ca XIX spectrum. Panel (c): variation of the electric field strength E (dotted line) and the ratio $\epsilon = E/E_D$ (solid line).

n, and E. In particular, given observational measurements of T and n, this ratio provides a novel diagnostic of the unknown electric field strength. We will exploit this diagnostic in the ensuing analysis.

For sub-Dreicer fields ($E << E_D$), the only electrons that runaway are those with velocities above a critical threshold velocity $v_c = (E_D/E)^{1/2} v_t$, where $v_t = (kT/m)^{1/2}$ is the thermal velocity. In this case, Joule heating will dominate since there are few electrons with velocities above v_c. Consequently, thermal soft X-ray emission will predominate relative to nonthermal high-energy hard X-rays. For increasing E/E_D, acceleration will dominate as a larger fraction of the electrons enter the runaway regime and produce increasing nonthermal HXR emission. Ultimately, all electrons will runaway when $E = E_D$. The dependence of increasing HXR emission on increasing $\dot{N}$ suggests the following relationship:

$$F_{HXR}/Q_{obs} \simeq \alpha \dot{N}/Q \qquad (2)$$

where the right-hand term is the theoretical ratio from equation (1), and the left-hand term is the ratio of the observed nonthermal HXR emission to the thermal heating rate implied by soft X-ray observations. The thermal heating rate is given by $Q_{obs} = dU/dt + P_r + P_c$ (Antonucci *et al.* 1984), where $U = 3nkTV$ is the total thermal energy, $P_r \approx 1.5 \times 10^{-19} n^2 T^{-1/2} V$ is the radiative energy loss rate, and $P_c \approx 10^{-6} T^{7/2} (2A/L)$ is the conductive loss rate for a symmetric loop with half-length L, constant cross-sectional area A, and total volume V.

Equation (2) depends only on the temporally-varying physical parameters T, n, and E, and a constant of proportionality α. The latter quantity effectively relates the observed HXR intensity F_{HXR} to the rate of acceleration of HXR-producing electrons. To a first approximation, we assume that: (1) α is constant during the flare; and (2) the density is related to the emission measure according to $n = (EM/V)^{1/2}$, where $V \approx 2AL$ is the loop volume (i.e., a unit filling factor). For the electric field strength, we assume a simple functional form in which E increases during the rise of impulsive hard X-rays and remains constant after the first peak of hard X-rays. Using T and EM from the Ca XIX spectral fits, and the loop geometry parameters from the Be-SXT images, we solve first for the magnitude of E and α after this first peak. We use a two parameter least-squares fit of equation (2) to the total (background-subtracted) HXR count rate above 50 keV measured by BATSE. Having solved for α at the peak, we subsequently derive the temporal variation of E during the HXR rise by numerically solving equation (2) backward in time with α held constant.

Figure 1c shows the results of the fitting process. We find that an electric field model with constant $E = 9 \times 10^{-5}$ volts cm^{-1} after the first HXR peak provides a good fit to the overall HXR evolution. Backward solution for the field strength during the rise phase indicates that the electric field increased by almost an order of magnitude from a preflare value of 10^{-5} volts cm^{-1}. It is instructive to examine the variation of the ratio $\epsilon = E/E_D$ during the flare. Figure 1c shows that ϵ increases sharply during the rise phase, peaking at $\epsilon = 0.18$ and decreasing rapidly thereafter. Note that the maximum value of ϵ is below the level at which turbulence-induced instabilities are expected to become pronounced (Tsuneta 1985). The initial rise in ϵ is due primarily to the increase in E and also to the increasing T produced by the current heating. Since E is assumed constant after the peak, the sharp drop in ϵ is due to the increase in the Dreicer field E_D caused by the increase in n. Physically, the increase in density acts to enhance collisional redistribution of thermal electrons, thereby quenching runaway acceleration and the associated nonthermal HXR emission. A similar result was found by Tsuneta (1985).

4. Conclusions

We have presented a new method for analyzing simultaneous soft and hard X-ray observations of solar flares. The method is based on the assumption that the temporal evolution of impulsive hard X-ray emission is physically related to the runaway acceleration rate of electrons in a DC-electric field. We have shown that the ratio of the electron runaway rate to the rate of Joule heating by a current is a straightforward function of the temperature, density, and electric field strength in the plasma. Using soft X-ray observations to infer temperature and density, we have solved for the unknown electric field strength.

Acknowledgements This work was supported by *Compton Gamma-Ray Observatory* Guest Investigator grant NAS5-32064 and by the Office of Naval Research.

References

1. Antonucci, E., Gabriel, A.H., and Dennis, B.R., 1984, *Ap. J.* **287**, 917.
2. Benka, S.G. and Holman, G.D., 1992, *Ap. J. (Letters)* **400**, L79.
3. Dreicer, H., 1959, *Phys. Rev.* **115**, 238.
4. Holman, G.D., 1985, *Ap. J.* **293**, 584.
5. Holman, G.D., Kundu, M., and Kane, S., 1989, *Ap. J.* **345**, 1050.
6. Moghaddam-Taaheri, E. and Goertz, C.K., 1990, *Ap. J.* **352**, 361.
7. Spicer, D. S., 1982, *Space Science Rev.* **31**, 351.
8. Tsuneta, S. 1985, *Ap. J.* **290**, 353.